Cement and Concrete Research 42 (2012) 1072–1082

Contents lists available at SciVerse ScienceDirect

Cement and Concrete Research

journal homepage: http://ees.elsevier.com/CEMCON/default.asp

Influence of the applied voltage on the Rapid Chloride Migration (RCM) test

P. Spiesz *, H.J.H. Brouwers

Department of the Built Environment, Eindhoven University of Technology, P.O. Box 513, 5600 MB Eindhoven, The Netherlands

ARTICLE INFO

Article history:
Received 18 October 2011
Accepted 19 April 2012

Keywords:
Concrete (E)
Chloride (D)
Diffusion (C)
Electrochemical properties (C)
Migration

ABSTRACT

This study addresses the influence of the applied voltage (electrical field) on the value of the chloride migration coefficient, as determined with the Rapid Chloride Migration (RCM) test, and on other properties of cement based mortars. It is shown that in the investigated ranges of applied voltages, the chloride migration coefficients, computed from two different chloride transport models, are relatively constant. However, other properties of mortars are changing due to the application of the electrical field. It is shown that the resistance of the test samples increases during the migration test (therefore the DC current during the test decreases). Moreover, the mass of the samples increases and this increase is found to be proportional to the chloride penetration depth. The pH of the catholyte solution (10% NaCl water solution) increases significantly during the migration test, thus the test conditions change as the OH^- to Cl^- proportion changes. Furthermore, the measured values of the polarization of the electrodes confirm the value of 2 V, assumed in the guidelines for the RCM test. Also, a dark coloration is observed on samples split after the test, prior to spraying with the colorimetric chlorides indicator. This coloration is attributed to a liquid-saturation of the samples only in the colored region and not in the entire volume of the sample, as is assumed after performing the vacuum-saturation prior to the migration tests.

1. Introduction

In the case of deteriorated concrete elements/structures being in frequent contact with a chloride bearing environment (e.g. de-icing salts or seawater), the chloride initiated corrosion of the reinforcing steel is the main reason of the deteriorations in the majority of cases. Therefore, a proper design of the concrete cover (the layer of concrete covering the steel), considering its quantity (thickness) and quality (permeability to chlorides), is very important from the point of view of service life and maintenance work. In order to quantify the chloride ingress speed in concrete, the chloride diffusion/migration coefficient is used, because the diffusion controls the ingress of chlorides. There are various laboratory test methods for determining the chloride diffusion/migration coefficient. In the past mainly the 'natural' diffusion test methods were used, in which concrete samples are exposed to a chloride solution for a long period, so the chlorides are penetrating the samples due to the concentration gradient. However, recently the application of electrically accelerated test methods has significantly increased due to their short testing period and simplicity. The Rapid Chloride Migration (RCM) test, described in the guideline NT Build 492 [1], is one of the accelerated test methods, which is nowadays very often used. The output of this test method—the chloride migration coefficient D_{RCM}—has been incorporated into the DuraCrete model [2] for the service life design of concrete structures. However, as demonstrated in Spiesz et al. [3], the D_{RCM}, computed according to the 'traditional' RCM model [1,4], has to be treated carefully because of oversimplifications of this theoretical model, which are reflected by the deviation of the chloride concentration profiles measured after the RCM test from the theoretical profiles. As shown in the improved RCM model [3], when taking into account the non-linear chloride binding isotherm and the non-equilibrium conditions between the free- and bound-chlorides (due to the short duration of the RCM test, which usually amounts to only 24 h), the transport of chlorides in concrete by migration can be predicted more accurately than given by the 'traditional' model.

Other important aspects regarding the chloride migration in concrete are the test conditions and their influence on the results of the test. According to the guideline for the RCM test [1], the value of the voltage applied during the test is adjustable, and depends upon the value of the initial current, which is measured at the DC voltage of 30 V. Based on the value of this current, which basically reflects the permeability of concrete (its permeability is related with its conductivity and therefore with the measured current), the value of the voltage applied during the RCM test and the duration of the test are adjusted, following Table 1 [1]. This action is performed in order to obtain a sufficient chloride penetration depth for concretes with low permeability, for which the initial voltage of 30 V would result in a too shallow chloride penetration depth, and to prevent the chloride breakthrough for concretes with high permeability (i.e. the chloride penetration depth obtained after the test should be within certain limits regardless of the permeability of concrete). As demonstrated in [4] and shown in

* Corresponding author. Tel.: +31 40 247 5904; fax: +31 40 243 8595.
E-mail address: p.spiesz@tue.nl (P. Spiesz).

0008-8846/$ – see front matter © 2012 Elsevier Ltd. All rights reserved.
doi:10.1016/j.cemconres.2012.04.007

Table 1
Applied voltage (U) and duration (t) of the RCM test, based on the initial current (I_{30}) measured at 30 V [1].

I_{30} [mA]	U [V]	t [h]
<5	60	96
$5 \le I_{30} \le 10$	60	48
$10 \le I_{30} \le 15$	60	24
$15 \le I_{30} \le 20$	50	24
$20 \le I_{30} \le 30$	40	24
$30 \le I_{30} \le 40$	35	24
$40 \le I_{30} \le 60$	30	24
$60 \le I_{30} \le 90$	25	24
$90 \le I_{30} \le 120$	20	24
$120 \le I_{30} \le 180$	15	24
$180 \le I_{30} \le 360$	10	24
≥360	10	6

Fig. 1 [4], a minimum penetration depth of about 10 mm is required in order to minimize the error (maximize the precision) of the chloride migration coefficient. As also demonstrated in [5], the resolution of the migration coefficient highly depends on the penetration depth of chlorides and is increasing when the penetration depth increases. The adjustable voltage and test duration imply that the testing conditions during the RCM test are not always the same. However, different test conditions may influence the test results. In the research of Stanish [6,7] it has been demonstrated that the chloride penetration depth is a linear function of the applied voltage and the duration of the RCM test. However, the migration coefficient was not investigated in that research, as the author believed that the RCM model developed by Tang [4] and the migration coefficients computed based on that model are doubtful. Therefore, the aim of this study is to evaluate whether the voltage applied during the RCM test is influencing the value of the chloride migration coefficient calculated based on two methods: the 'traditional' RCM model [1,4] and the RCM model presented recently by Spiesz et al. [3]. Additionally, other measurements (such as mass, electrical resistance, DC current, etc.) are performed in order to demonstrate whether the applied voltage has any influence on the properties of the test samples, the electrolytes and the polarization potential of the electrodes.

2. Materials and methods

2.1. Materials and mixture design

A mortar was used in this study to investigate the influence of the applied voltage on the RCM test, because mortars do not contain coarse aggregates which are impermeable to chlorides and therefore often disrupt the chloride penetration front. Fig. 2 shows the differences between chloride penetration fronts that can usually be observed after the RCM

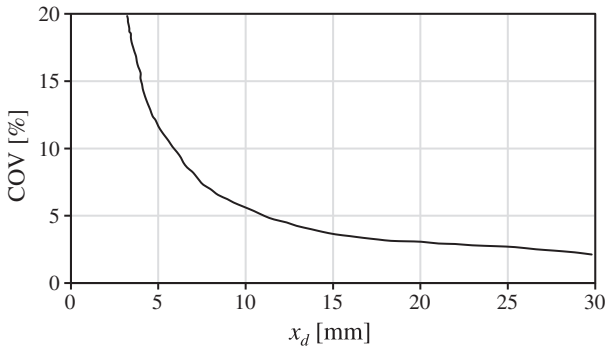

Fig. 1. Coefficient of variation (COV) introduced to the value of D_{RCM} by measurement of the chloride penetration depth x_d ($U=30$ V, $L=0.05$ m, $T=298$ K, $t=24$ h, $c_0=2$ mol/dm^3 and the accuracy of x_d measurement of ±0.5 mm) [4].

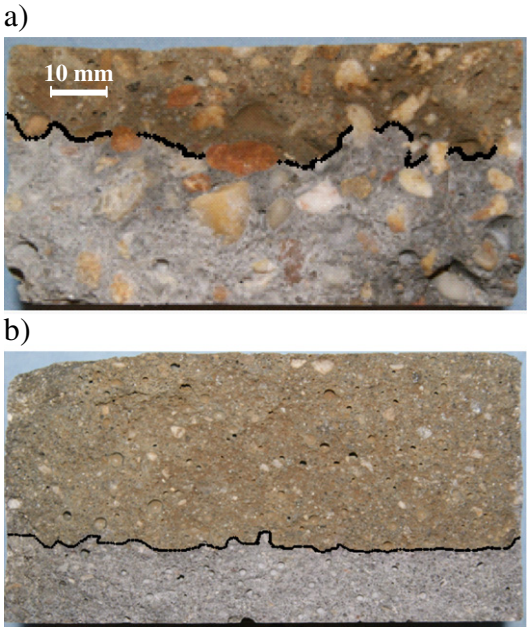

Fig. 2. Typical chloride penetration fronts after the RCM test observed on: a) concrete and b) mortar.

test on concretes and mortars. A uniform chloride penetration front (Fig. 2b) will help to reduce discrepancies in measurements of the chloride penetration depths and the total chloride concentration profiles.

As mentioned earlier, NT Build 492 [1] recommends applying a voltage in the range of 10–60 V, depending on the value of the initial current, recorded when a voltage of 30 V is applied. Therefore, in order to compare the chloride migration coefficients obtained for different voltages, the mortar used in this study is intended to have 'average' permeability according to NT Build 492. Here, the 'average' permeability represents such a permeability of mortar, for which according to Table 1 [1] the initial current at voltage of 30 V should be in the middle range of the given initial currents (20–60 mA), so that the same mortar recipes tested at $U=30$–40 V could also be tested using higher and lower voltages, without a risk of chloride breakthrough or very shallow chloride penetration depth, respectively.

In order to find a mortar of 'average' permeability, in preliminary experiments a few mortars of different quality (and permeability), obtained by varying the content of cement and the water–cement ratio, were cast in 150 mm cubes. The mortars were composed of Portland cement CEM I 52.5 N, sand 0–2 mm, water and polycarboxylate-based superplasticizer. One day after casting, the cubes were demolded and then cured in water until the age of 27 days, when the cylindrical cores were extracted from the cubes by drilling, cut and saturated with limewater under vacuum conditions. At the age of 28 days the samples were placed in the migration test set-up and the initial current at the external voltage of 30 V was measured, so that the RCM test conditions for these mortars could be specified following Table 1. Based on these trials, the mortar mixture shown in Table 2 was selected for further testing and subsequently a new set of nine cubes (150 mm size) was cast,

Table 2
Composition of the employed mortar mixture.

Material	Volume [dm^3]	Mass [kg/m^3]
CEM I 52.5 N	249.4	785.6
Sand 0–2 mm	521.5	1382.1
Superplasticizer (SP)	7.1	7.86
Water (including water from SP)	206.9	206.9
Air	20	–
Total	1000	2377.4

demolded after one day and cured in water. Three of these cubes were tested for their compressive strength at the age of 28 days and a mean value of 97.8 N/mm^2 was recorded. This high strength can be explained by a high cement content and low *w/c* ratio in the mix.

2.2. Rapid Chloride Migration test

Six cylindrical cores ($\Phi = 100$ mm) were extracted from the remaining mortar cubes at the age of 27 days. From these cores 12 specimens of 50 mm in height were sliced for the RCM test (two specimens from each core, 10–20 mm of the outermost surfaces of each core were cut off) and stored in water. One day prior to the RCM test, each series of the test samples was saturated with limewater under vacuum conditions. The vacuum-saturation was performed following the procedure described in [1,8]: surface-dry samples were placed vertically in a desiccator connected to a vacuum-pump and a pressure of 40 mbar was applied for 3 h. Then, with the vacuum-pump still running, the desiccator was slowly filled with limewater to immerse all the samples completely. After that, for an additional hour, the vacuum was maintained before allowing air to re-enter the desiccator. The samples were kept in the solution for about 18 h. The RCM test was performed on the saturated samples at the age of 28, 29 and 30 days. Power sources with constant voltage outputs (adjustable in the range of 0–80 V, accuracy of 0.05 V) were used. The scheme of the RCM test set-up is shown in Fig. 3. Four mortar samples were tested at the same time. The used volume of the catholyte (10% NaCl aq. solution) was about 14 l while the volume of the anolyte (0.3 M NaOH solution) was approximately 0.3 l per test specimen. The electrolytes were refreshed after each series of experiments. After the migration test, three mortar samples were split and sprayed with a 0.1 M $AgNO_3$ solution in order to determine the penetration depth of chlorides, while the total chloride concentration profile was measured on the fourth sample.

In order to investigate the influence of the applied voltage on the chloride migration coefficient, three series of mortar specimens were tested at three different voltages. According to the plan of the experiment, a mortar of 'average' permeability according to Table 1 ($20 < I_{30} < 60$ mA; hence U in the range of 30–40 V) was prepared. Besides testing the mortar at the voltage of $U = 30$–40 V, also tests at the voltages $U + 20$ V and $U - 20$ V were planned. However, as will be explained later, this initial plan had to be modified due to the very shallow chloride penetration depths obtained in the first experiments.

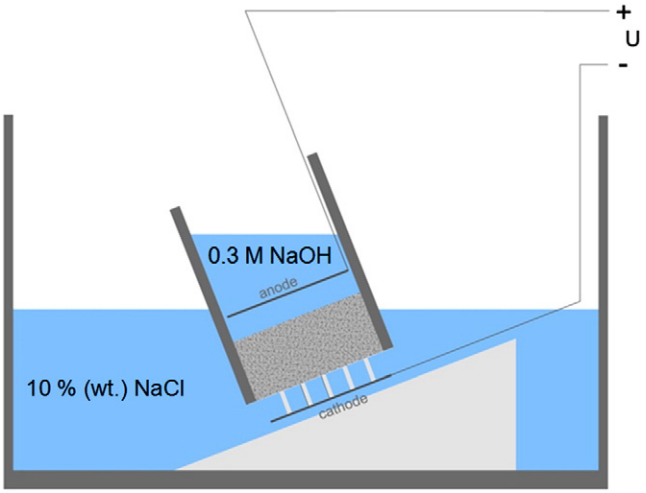

Fig. 3. RCM test set-up.

2.3. Chloride concentration profile measurements

Immediately after finishing the RCM test, the mortar samples were ground in layers. A surface layer of 0.5 mm was ground at first and then 1 mm layers were ground consecutively, until a depth of approximately 5 mm farther than the chloride penetration depth measured previously on split samples (by the $AgNO_3$ colorimetric method) was achieved. The grinding process was finished 2–3 h after finishing the RCM test. About 4 g of mortar dust was collected from the surface layer and about 8 g from each deeper layer. Afterwards, the dust was sieved on a 0.25 mm sieve (in practice, all the ground material is passing this sieve). Subsequently, this passing fraction was dried in a ventilated oven at 105 °C, until a constant mass was reached. In order to extract the chlorides, 2 g of dried powder from each analyzed layer was poured into a beaker together with 35 ml of distilled water and 2 ml of 1 M HNO_3, shaken manually for 1 min and heated up to reach the boiling point. Next, the solution was cooled down, filtered, and its volume was adjusted to 100 ml by adding distilled water. 10 ml samples were analyzed for the chloride concentration by using an automatic potentiometric titration unit and 0.01 M $AgNO_3$ solution as the titrant. The measured concentration was expressed as the mass of chlorides in 100 g of dry mortar. The minimum chloride concentration (C_{bi}—the background concentration) which could be measured by the titration unit was 0.03 $g_{Cl}/100\ g_{mortar}$.

2.4. Polarization potential measurements

The polarization potential of the electrodes is included in the formulas for calculating the D_{RCM} coefficient in NT Build 492 [1] and amounts to 2 V. In [9] the measured values of the polarization potential of the stainless-steel electrodes used in the Rapid Chloride Permeability test (RCPT) [8] are given. The cumulative values of the polarization potential for both electrodes are reported to be in the range of 1.91–2.36 V for the applied external voltage of 6 up to 30 V. However, the test set-up for the RCPT test is different than the test set-up employed for the RCM test (e.g. electrolytes and their volumes or applied voltages), so the polarization potential during the RCM test may vary from the values reported in [9].

In order to measure the polarization potential of the electrodes during the RCM test, a circuit built as shown in Fig. 4 was used. The potentiodynamic measurements were performed on stainless steel

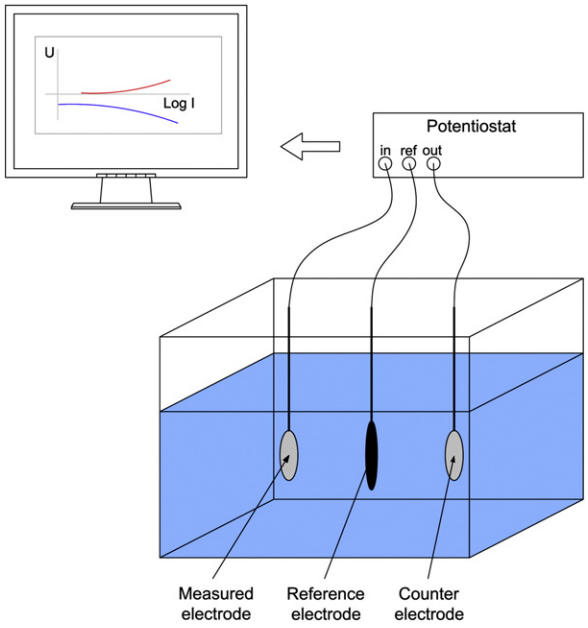

Fig. 4. Test set-up for measurements of the polarization of the electrodes.

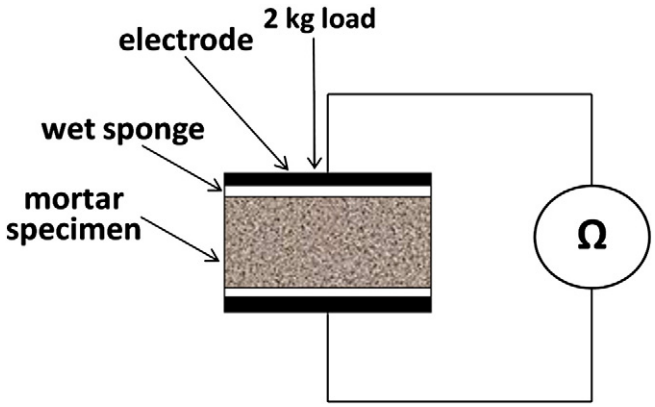

Fig. 5. Test set-up for measurements of the electrical resistance of the mortars.

electrodes (SS) as well as on mixed-metal-oxides coated titanium (MMO-Ti) electrodes. The MMO-Ti electrodes were tested as the titanium is an ideal material for the electrodes (high resistance against corrosion). A scan rate of ±0.056 mV/s was used. A standard reference Ag|AgCl electrode and MMO-Ti as the counter electrode were employed. The polarization measurements were performed in the anolyte solution (0.3 M NaOH) for the anode and in the catholyte solution (10% NaCl) for the cathode.

2.5. Additional measurements

The DC current was measured continuously on one specimen for each experimental series using a digital multimeter (accuracy of 0.01 mA) in a serial connection. The current was logged in a five-minute step during the migration experiments. The resistance was measured using a commercial LCR meter (accuracy of 2%, frequency of the test AC signal: $f = 1$ kHz). The 'two electrodes method' (Fig. 5) was used for measuring the electrical resistance of the mortar samples before/after the vacuum-saturation and after the migration test. A load of 2 kg was applied during the measurements in order to obtain reproducible results. The pH of the catholyte and anolyte solutions was measured periodically during the migration test. The pH meter (accuracy of 0.01) was calibrated in the pH range of 4–14. The mass of the samples was measured prior to and after the vacuum-saturation and after the RCM test using a technical balance with an accuracy of 10 mg. The water-accessible porosity was measured on mortar discs ($\Phi = 10$ cm, $h = 1$ cm), extracted from the inner layers of the mortar cubes. The discs were water-saturated under vacuum conditions at the age of 28 days, following the same procedure as described earlier for the RCM test samples. Afterwards the mass of the saturated samples was measured in air (in surface-dry conditions) and in water. Next, the samples were dried in an oven at 105 °C until a constant mass was reached and then weighted. Finally, the porosity was calculated according to the following equation [10]:

$$\varphi = \frac{m_s - m_d}{m_s - m_w} \times 100, \quad (1)$$

where: φ—porosity, m_s—mass of water-saturated sample in air, m_w—mass of water-saturated sample in water and m_d—mass of dried sample.

3. Results and discussion

3.1. Chloride penetration depth

The application of the electrical field lasted 24 h in all the experiments. After testing each series of four mortar samples using the RCM test set-up, three samples were split and sprayed with $AgNO_3$—a colorimetric indicator for chlorides. AgCl, being the product of the reaction of $AgNO_3$ with chlorides, has a white color, while AgOH (which is later transformed to Ag_2O), formed in the chloride-free regions of sample, is brownish. Therefore, the boundary between the regions with and without chlorides becomes clearly visible and the chloride penetration depth can be measured.

As expected, in all the investigated samples the chloride penetration fronts were straight and not distorted because no large aggregates were present in the mortars (see Fig. 6a–c). As explained earlier (see Section 1 and Fig. 1), ideally the chloride penetration depths after the RCM test should be greater than 10 mm, therefore the voltage and the duration of the RCM test are adjusted based on the initial value of the current at the voltage of 30 V. As planned, the initial currents measured at 30 V on mortar samples were in the target range of 20–60 mA (I_0 of about 31 mA). Hence, for the first series of samples, the voltage U of 35 V (according to Table 1 for the measured I_0) was applied and a chloride penetration depth greater than 10 mm was expected. However, as can be seen in Fig. 6a, the measured depths were lower, about 8.5 mm in average. In order to obtain more significant chloride penetration depths, the experimental plan was modified and for the two other series of experiments higher voltages were applied (47.5 V and 60 V respectively), as can be seen in Table 3. Table 1 [1], which was developed based on experience with OPC concrete, could not provide such test conditions that would result in the desired chloride penetration depths for the tested mortar (from the practical experience of the authors, a similar problem often occurs also for concrete based on CEM III). Moreover, as mentioned

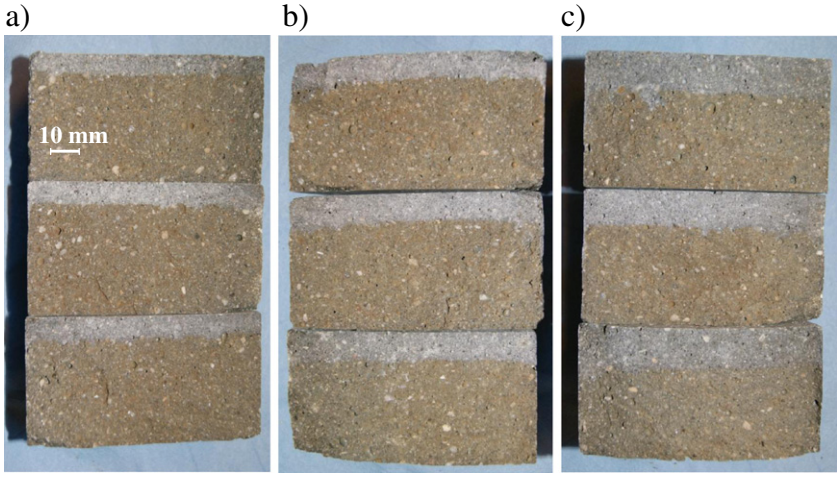

Fig. 6. Chloride penetration depths in mortars: a) 35 V; b) 47.5 V; c) 60 V.

Table 3
DC currents measured during the RCM tests.

Sample number	U [V]	Current [mA]			
		At 30 V, I_{30}	Initial at U, I_0	Final at U, I_f	Decrease [%]
1	35.0	30.41	35.41	33.23	6.2
2	35.0	31.57	37.40	35.55	4.9
3	35.0	31.12	36.90	34.37	6.9
4[a]	35.0	30.17	35.72	33.43	6.4
5	47.5	30.18	48.95	47.14	3.7
6	47.5	30.34	49.25	47.53	3.5
7	47.5	30.14	49.05	47.46	3.2
8[a]	47.5	29.75	47.87	44.37	7.3
9	60.0	30.43	62.60	61.87	1.2
10	60.0	31.21	64.26	63.76	0.8
11	60.0	31.45	64.81	63.87	1.4
12[a]	60.0	29.07	62.20	60.47	2.8

[a] Current registered continuously during 24 h.

in NT Build 492 [1], if specimens with a high content of cement are tested, the current measured at $U = 30$ V should be multiplied by a factor equal to the ratio of normal binder content to actual binder content, in order to be able to use Table 1. This means in practice that much lower voltages should be used to test samples with a high content of cement. Following this recommendation, the penetration depth obtained on the mortars tested in this study would be even lower, reducing the precision of the D_{RCM} (see Fig. 1).

As can be seen in Fig. 7, the measured penetration depth of chlorides can be correlated with a linear function to the applied voltage with a good accuracy in the investigated range of voltages ($R^2 = 0.95$). This conclusion is in line with results presented by Stanish in [6,7].

3.2. Polarization potential of the electrodes

The potentiodynamic measurements of the polarization potential were performed on the stainless steel electrodes (SS), which were used in the RCM test set-up (Fig. 3), as well as on the mixed-metal-oxides coated titanium (MMO-Ti) electrodes. The absolute values of measured potentials are shown in Fig. 8a for the SS electrodes and in Fig. 8b for the MMO-Ti electrodes. The total polarization potential, which is equal to the sum of the polarizations of both electrodes, is also shown in Fig. 8a–b, but only in the range of 10 up to 100 mA, as this is the usual range of the DC currents flowing during the RCM test [1]. As can be seen, for the SS electrodes, the total polarization potential holds in the range of 1.8 up to 2.2 V, which confirms the assumption of 2 V adopted in NT Build 492 [1] and is in line with the results presented in [9]. For the MMO-TiO_2 electrodes this potential is slightly lower and holds in the range of 1.5 up to 1.8 V. Besides their excellent corrosion resistance, using the Ti-MMO electrodes in the RCM test set-up could help to reduce the error introduced to the D_{RCM} coefficients in the guidelines for the RCM test, which do not take the polarization effect into account (e.g. [11]).

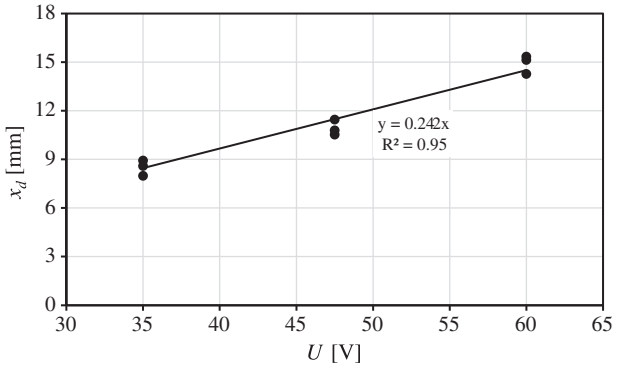

Fig. 7. Chloride penetration depth (x_d) vs. applied voltage (U).

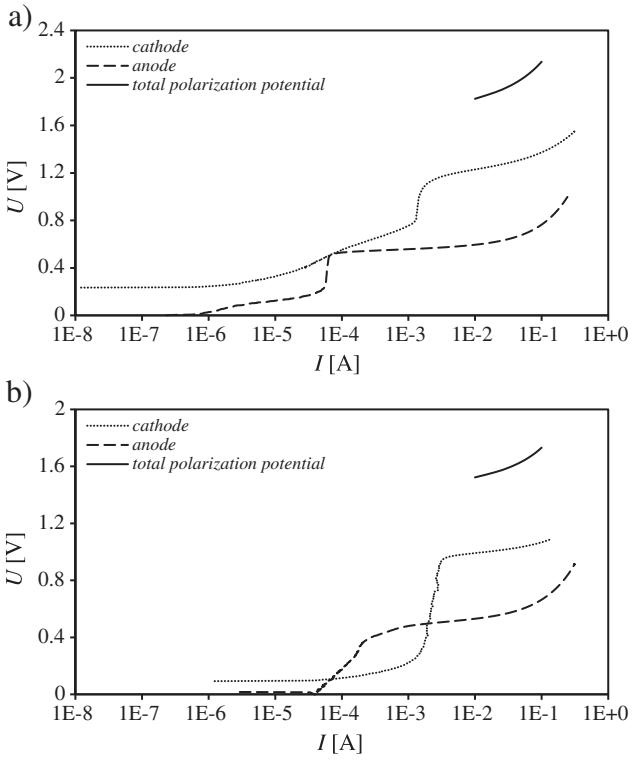

Fig. 8. Polarization potential of the electrodes: a) SS; b) MMO-Ti.

3.3. DC current and resistance

Table 3 presents the values of DC currents measured at 30 V (I_{30}) and the initial and final currents measured during the RCM test (I_0 and I_f respectively). For one sample of each test series the current was registered continuously during 24 h of the RCM test and this data is shown in Fig. 9.

Table 4 shows the electrical resistance of test samples (measured before and after vacuum-saturation and after the RCM test) and the resistance of the system mortar-electrolyte-electrode calculated from Ohm's law (for the measured I_0 and I_f). Analyzing the results shown in Table 4, one can notice that after the vacuum-saturation, the resistance of mortar samples decreases; this can be attributed to

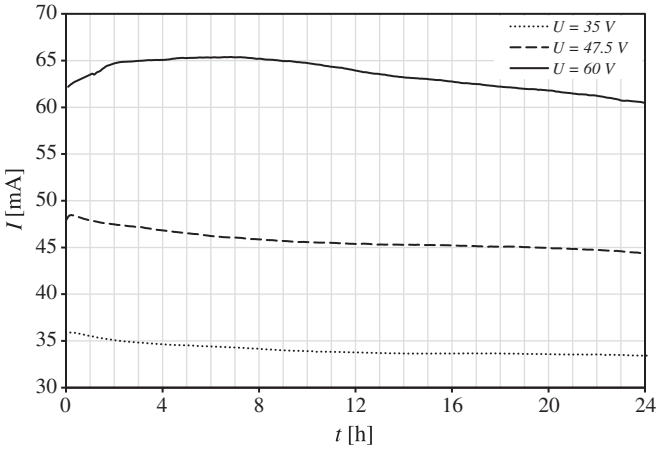

Fig. 9. DC current during the RCM test for the applied voltage.

Table 4
Measured and calculated resistance of the samples.

Sample number	Resistance [Ω]				
	Before saturation	After saturation	After RCM test	Calculated from I_0	Calculated from I_f
1	912	821	1039	988	1053
2	907	825	1028	936	985
3	898	815	1039	948	1018
4	872	818	1020	980	1047
5	905	802	948	970	1008
6	936	803	953	965	999
7	904	812	937	968	1001
8	929	832	957	992	1071
9	885	824	1097	959	970
10	867	801	1029	934	941
11	870	818	997	926	939
12	878	815	998	965	992

the pores that become filled with liquid. Interestingly, the opposite effect can be observed during the RCM test—the resistance of test samples increases of about 25% during the test. Analyzing the data shown in Table 3 and in Fig. 9 it can be noticed that the DC current decreases during the migration test, which corresponds to the increase of resistance of the tested samples. This increase in resistance can be attributed to a densification of the pore system due to chloride binding—as suggested in [12,13], to a partial replacement of OH^- by free-chlorides in the pore solution, which causes its lower conductivity (OH^- has a higher mobility compared to Cl^- [14]) or to the leaching of e.g. Ca^{2+} and K^+ ions from the sample into the catholyte solution.

As can also be observed in Fig. 9, the evolution of current during the RCM test is similar for $U = 35$ V and 47.5 V—it is characterized by an increase in the first 30 min of the test and then by a continuous drop until the end of the test. However, this behavior is different for $U = 60$ V, where the current increases for a longer time (until approximately 7 h), and then drops. Here it is important to mention that there was no increase of the temperature observed in the migration cell at any applied voltage.

3.4. pH of electrolytes, mass and porosity of test samples

Fig. 10 shows the evolution of pH in the catholyte and anolyte solutions, measured periodically during the RCM test. It can be noticed that not only the properties of the test samples change during the test (as discussed in the previous section), but there are also continuous changes in the composition of the electrolytes, due to the flowing

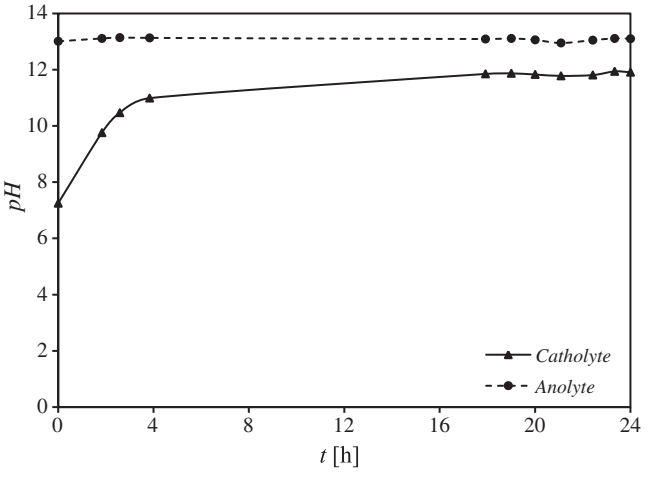

Fig. 10. pH evolution in electrolytes during the RCM test.

Table 5
Porosity measurements.

Sample number	Mass [g]			Porosity φ [%]
	Saturated, in air, m_s	Saturated, in water, m_w	Dry, in air, m_d	
3	176.16	101.80	164.92	15.11
6	226.89	131.53	212.69	14.89
9	228.90	132.49	214.40	15.04

currents and electrochemical processes at the electrodes. The pH measured in the NaOH solution (anolyte) remains constant during the RCM test, which means that the consumption of the OH^- ions at the anode is balanced by the inflow of these ions from the mortar samples into the solution. However, on the cathodic side, the pH level rises from about 7 to about 12 during the RCM test (i.e. the OH^- concentration increases by five orders of magnitude during 24 h). This means that, at the end of the test, a larger fraction of the current is carried by the OH^- ions than by the Cl^- ions, compared to the initial conditions when the concentration of OH^- was very low.

The porosity was calculated from Eq. (1), following measurements of the mass of water-saturated samples in air and in water and the mass of dry samples. The measurement results are presented in Table 5 and are showing a good reproducibility. The obtained porosity values may be underestimated if the vacuum-saturation with liquid was not sufficient to fill in all the pores with water. However, to minimize the influence of a dense microstructure of the prepared mortar (due to the low *w/c* ratio) on the efficiency of the vacuum-saturation technique, thin slices (about 10 mm in height) were used for the measurements.

The mass of the samples prior to and after the vacuum-saturation and after the RCM test is presented in Table 6. The mass increase due to the vacuum-saturation amounts to 0.07–0.12% (0.6–1 g), whereas the mass change during the RCM test is more significant and amounts to 0.16–0.37% (1.5–3 g). Fig. 11 shows a linear relationship between the mass increase of the sample during the RCM test and the average chloride penetration depth. This increase of mass cannot be fully explained by the fact that the Cl^- ions, which are replacing part of the OH^- ions in the sample (there is Cl^- and OH^- inflow but only OH^- outflow), have a larger molar mass. The amount of chlorides replacing the hydroxyl ions in the sample and the resulting increase of the mass can be estimated. Assuming that there are no other anions in the system (or their mobility is much lower compared to Cl^- and OH^-), the number of OH^- ions replaced in the sample by the Cl^- ions is equal to the number of the Cl^- ions which entered the sample from the external solution during the RCM test, following the charge conservation law. The total amount of the chlorides which entered into the sample can be calculated by averaging the chloride contents from the total concentration profiles (presented in Section 3.5) over

Table 6
Measured mass of the mortar samples.

Sample number	Mass [g]			Mass increase [%]	
	Before saturation	After saturation	After RCM test	After saturation	After RCM test
1	901.72	902.46	904.22	0.08	0.20
2	912.46	913.43	914.92	0.11	0.16
3	906.90	907.78	909.49	0.10	0.19
4	893.24	894.03	895.55	0.09	0.17
5	907.07	907.70	910.70	0.07	0.33
6	912.89	913.62	915.74	0.08	0.23
7	906.76	907.49	909.93	0.08	0.27
8	907.07	907.98	910.13	0.10	0.24
9	910.18	911.27	914.48	0.12	0.35
10	907.56	908.47	911.78	0.10	0.36
11	907.95	908.77	912.11	0.09	0.37
12	906.23	907.14	910.05	0.10	0.32

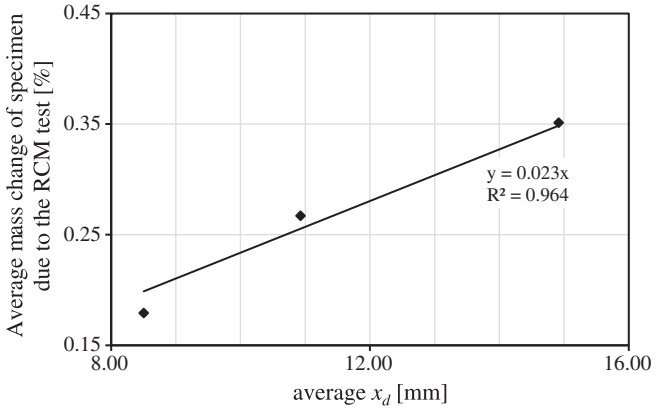

Fig. 11. Mass increase of samples vs. the chloride penetration depth (x_d).

the chloride penetration depth. Table 7 shows the calculated chloride amounts which penetrated into the sample during the test, the equivalent OH^- amounts which were replaced by the chlorides and the corresponding difference of mass. As can be seen, the calculated mass differences do not explain the differences measured between the mass of samples prior to and after the RCM test. Additionally, the increase of the mass of the sample by OH^- replacement with Cl^- ions is probably diminished by the fact that the Ca^{2+} ions are replaced in the sample with the Na^+ and/or H^+ ions, which are generated at the anode in the electrolysis of water. Therefore, it can be concluded that the increase in the mass of the samples during the RCM test is caused by different processes than a simple ionic exchange. Although this still needs further verifications, after proper calibration the mass change of the test sample during the RCM test could be related to the D_{RCM} coefficient, without applying the $AgNO_3$ chloride-indicator and the D_{RCM} computation steps.

In all the analyzed mortar samples a darker region was observed from the side of exposure to chlorides (Fig. 12a) after splitting and prior to spraying with $AgNO_3$. The depth of this region was comparable to the chloride penetration depth indicated by $AgNO_3$ (Fig. 12b). To the authors' knowledge, this phenomenon has not been reported in literature yet for the RCM test. Although the test sample should be liquid-saturated in its entire volume, as assumed after performing the vacuum-saturation, the most likely reason of the dark region is the liquid-saturation only in that region, but not due to the vacuum-saturation but due to the RCM test and the applied electrical field (electro-osmosis). The dark coloration vanishes in a few minutes after splitting the sample, and therefore is attributed to the evaporation of water. The microstructure of the mortar analyzed in the present study is rather dense (low w/c ratio and high content of cement) and therefore the sample could remain not fully saturated with liquid after performing the vacuum-saturation. However, from the experience of the authors, the dark coloration region can be observed on the split RCM samples regardless from the quality (permeability) of the tested material. To demonstrate that, a split concrete sample of 'an average' quality (age of 28 days, $w/c = 0.5$, $U = 30$ V, 28 days compressive strength of 54.5 MPa), prior to and after applying $AgNO_3$, is shown in Fig. 12c–d, where a similar dark coloration can be found.

If confirmed, the non-saturated state of the test samples would question all the current migration models (in all of them mortar/concrete samples are considered to be fully saturated) and thus, this issue needs further investigation.

Table 7
Estimated change of the mass of the test samples due to ionic exchange.

U [V]	35	47.5	60
Average x_d [mm]	8.5	10.9	14.9
ρ_d [kg/m^3]	1955	1955	1955
Average C_t [g_{Cl}/100 g_{mortar}]	0.52	0.55	0.61
m_{Cl} [g]	0.68	0.92	1.40
n_{Cl} [mol], n_{OH} [mol]	0.019	0.026	0.039
m_{OH} [g]	0.33	0.44	0.67
$m_{Cl} - m_{OH}$ [g]	0.35	0.48	0.73
Measured average Δm [g]	1.62	2.43	3.19

3.5. Total chloride concentration profile

The measured total chloride concentration profiles are shown in Fig. 13. In all of these profiles the concentration of chlorides decreases gradually from the maximum at the surface to zero. This contradicts the abrupt shape of the theoretical chloride concentration profile following the 'traditional' RCM model, and is compatible with the shape of experimental chloride concentration profiles measured by many other researchers [1,6,7,15–23]. The average values of the chloride penetration fronts (x_d), measured by the colorimetric method on sister samples, are also depicted in Fig. 13. It can be seen that for all measured profiles, the x_d was indicated at a total chloride concentration of approximately 0.1 g_{Cl}/100 g_{mortar}, which is in line with the values given by Stanish [7] for OPC concrete, and also corresponds well to the value of 0.07 mol/dm^3 reported by Otsuki et al. [24].

3.6. D_{RCM} coefficient

The D_{RCM} coefficients were calculated following the 'traditional' RCM model [1,4] as follows:

$$D_{RCM} = \frac{RTL}{zF(U-2)} \times \frac{x_d - \alpha\sqrt{x_d}}{t_{RCM}}, \tag{2}$$

where: R—universal gas constant [8.314 Jmol^{-1} K^{-1}], T—temperature [293 K], L—thickness of the sample [0.05 m], U—applied external voltage, z—ion valance, F—Faraday constant [96,485 C/mol], x_d—average chloride penetration depth, α—laboratory constant and t_{RCM}—duration of the test [s]. The laboratory constant α is calculated as follows:

$$\alpha = 2\sqrt{\frac{RTL}{zF(U-2)}} \times erf^{-1}\left(1 - \frac{2c_d}{c_0}\right), \tag{3}$$

where: c_d—minimum free-chloride concentration at which the colorimetric indicator changes the color [0.07 $mol_{Cl}/dm^3_{solution}$] and c_0—concentration of chlorides in the bulk solution [64.95 $g_{Cl}/dm^3_{solution}$ = 1.83 $mol_{Cl}/dm^3_{solution}$].

The calculated values of the D_{RCM} coefficients are shown in Table 8. It can be noticed that for the applied voltage of 35 V and 47.5 V the calculated average values of the D_{RCM} are almost identical and for the voltage of 60 V they are slightly increased (about 10%). This shows that the obtained chloride migration coefficients are rather independent from the values of the voltages in their investigated range.

Fig. 14 shows the theoretical free-chloride profiles computed from the 'traditional' RCM model as follows [4]:

$$c = \frac{1}{2}c_0\left[erfc\left(\frac{x - aD_{RCM}t}{2\sqrt{D_{RCM}t}}\right) + e^{ax}erfc\left(\frac{x + aD_{RCM}t}{2\sqrt{D_{RCM}t}}\right)\right], \tag{4}$$

where $a = zF(U-2)/(RTL)$, and c_0—concentration of chlorides in the bulk solution [$g_{Cl}/dm^3_{solution}$].

For the computation of the theoretical chloride concentration profiles, the average values of the D_{RCM} coefficients shown in Table 8 were used in Eq. (4).

As can be found in [4], the D_{RCM} in Eq. (4) is taking a linear chloride binding isotherm into account, i.e. $D_0/(\delta c_b/\delta c) = \text{constant} = D_{RCM}$. When accepting this assumption of linear binding, it could be noticed that the binding of chlorides will influence the values of the measured

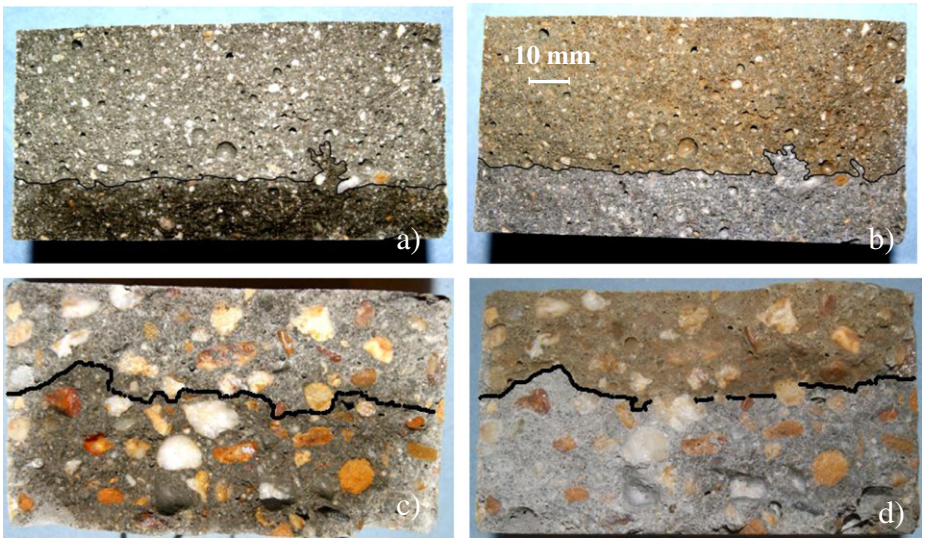

Fig. 12. Mortar sample before (a) and after (b) spraying with $AgNO_3$; Concrete sample before (c) and after (d) spraying with $AgNO_3$.

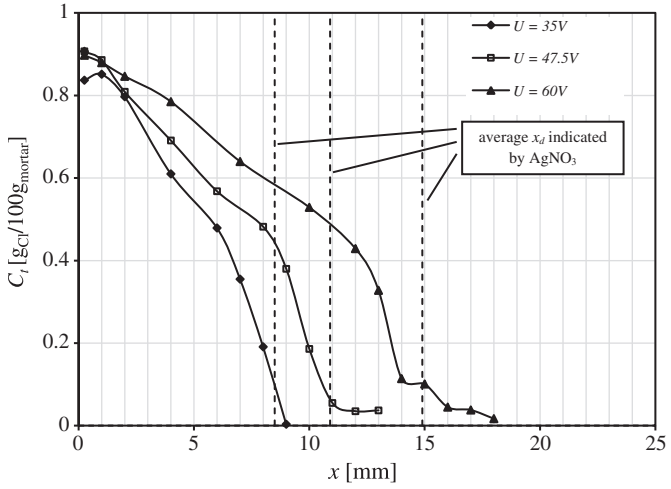

Fig. 13. Total chloride concentration profiles (C_t) measured after the RCM test.

total chloride concentration profile (as the total chloride concentration equals the sum of the free- and bound-chlorides concentrations), but will not alter the shape of the total chloride concentration profile. Therefore, as shown in Fig. 14, the measured total chloride concentration profiles can be translated into the free-chloride concentration profiles from a proportion, assuming that the free-chloride concentration in the exposed surface layers of the tested mortars equals to the bulk solution concentration ($c_0 = 64.95$ g/dm^3). As it is shown in Fig. 14, when comparing the theoretical free-chloride concentration profile (calculated from Eq. (4)) to the free-chloride profile calculated from the measured total chloride concentration profile, one can notice that the 'traditional' theoretical RCM model cannot predict the transport of chlorides in concrete/mortar accurately, which is in line with the data shown in [1,3,6,7,15–23].

Table 8
D_{RCM} calculated following NT Build 492.

Sample number	U [V]	x_d [mm]	D_{RCM} [$\times 10^{-12}$ m^2/s]	D_{RCM} - average [$\times 10^{-12}$ m^2/s]
1	35.0	8.9	3.31	
2	35.0	8.6	3.15	3.11
4	35.0	8.0	2.87	
5	47.5	10.8	3.04	
7	47.5	11.5	3.25	3.09
8	47.5	10.5	2.97	
10	60.0	15.1	3.47	
11	60.0	15.3	3.51	3.41
12	60.0	14.3	3.26	

3.7. D_{eff} coefficient

As demonstrated in [3], the binding term ($\delta c_b/\delta c$) is not constant and therefore the D_{RCM} coefficient is inaccurate, because it takes this binding term into account as a constant value (see Section 3.6). For this reason, the effective chloride migration coefficient (D_{eff}), which is independent from the binding term, was adopted in the new RCM chloride transport model [3]. This coefficient is dependent only on the diffusivity of chlorides in free liquid and on the pore structure of the material. Because of the difference in consideration of the binding term, the D_{RCM} and the D_{eff} are not equal to each other and their direct comparison cannot be performed without significant simplifications (an example of such comparison is shown in [3]).

Following the chloride transport model given in [3], the non-linear chloride binding isotherm and the non-equilibrium conditions

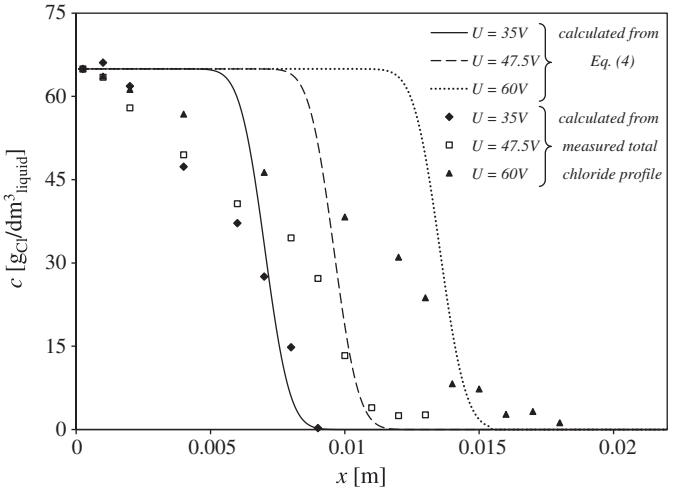

Fig. 14. Free-chloride concentration profiles computed according to the traditional RCM model [4] and calculated from the measured total chloride profiles.

Table 9
Parameters obtained from the new RCM chloride transport model given in [3].

Sample number	U [V]	D_{eff} [$\times 10^{-12}$ m^2/s]	k [$\times 10^{-6}$ 1/s]	K_b [$\times 10^{-4}$ dm^{3n}/g^n]	n
3	35.0	0.74	4.7	6.7	0.50
6	47.5	0.64	4.9	6.9	0.51
9	60.0	0.81	5.3	6.9	0.50

between the free- and bound-chlorides were taken into account. Except for these differences in the binding of chlorides, the other main assumptions of the new RCM model are the same as for the 'traditional' RCM model [4]: i) migration of chlorides due to the electrical field is much greater compared to the diffusion due to the concentration gradient, ii) neglected influence of other ions, iii) one dimensional and linear electrical field distribution across the sample and iv) constant properties of the sample and constant conditions during the test. The developed system of equations for liquid and solid states respectively reads [3]:

$$\varphi\frac{\delta c}{\delta t}+D_{eff}\frac{zFU}{RTL}\frac{\delta c}{\delta x}=-k\left[c-\left(\frac{C_b}{K_b}\right)^{1/n}\right] \tag{5}$$

$$(1-\varphi)\times\rho_S\frac{\delta C_b}{\delta t}=k\left[c-\left(\frac{C_b}{K_b}\right)^{1/n}\right], \tag{6}$$

with the following initial and boundary conditions:

$$\begin{aligned} c(x=0,t)&=c_0\\ C_b(x,t=0)&=C_{bi}, \end{aligned} \tag{7}$$

where: c—free-chloride concentration [$g_{Cl}/dm^3_{solution}$], C_b—bound chloride concentration [g_{Cl}/g_{mortar}] and c_0—concentration of chlorides in the bulk solution [$g_{Cl}/dm^3_{solution}$].

Applying the numerical solution of this model [3] to the experimental data ($c_0=64.95$ g/dm^3, apparent density of liquid-saturated mortar $\rho_c=2450$ g/dm^3, specific density of mortar $\rho_s=2710$ g/dm^3, porosity values in Table 5, voltage values in Table 3) and to the measured total chlorides concentration profiles, the effective chloride migration coefficient (D_{eff}), the chloride mass transfer coefficient (k) and the chloride binding parameters of the Freundlich isotherm (K_b—binding capacity and n—binding intensity) were estimated by using an optimization procedure described in [3]. All the optimized values are given in Table 9 and the generated total chloride concentration profiles are shown in Fig. 15a–c. It can be seen that the obtained values of the D_{eff} are within the range of $0.64–0.81\times10^{-12}$ m^2/s and there is no clear trend regarding the value of applied voltage. The obtained values of the Freundlich isotherm parameters are in line with experimental binding measurements on OPC mortar shown in [4], recalculated to the units used in this study ($K_b=5.3\times10^{-4}$ dm^{3n}/g^n and $n=0.52$).

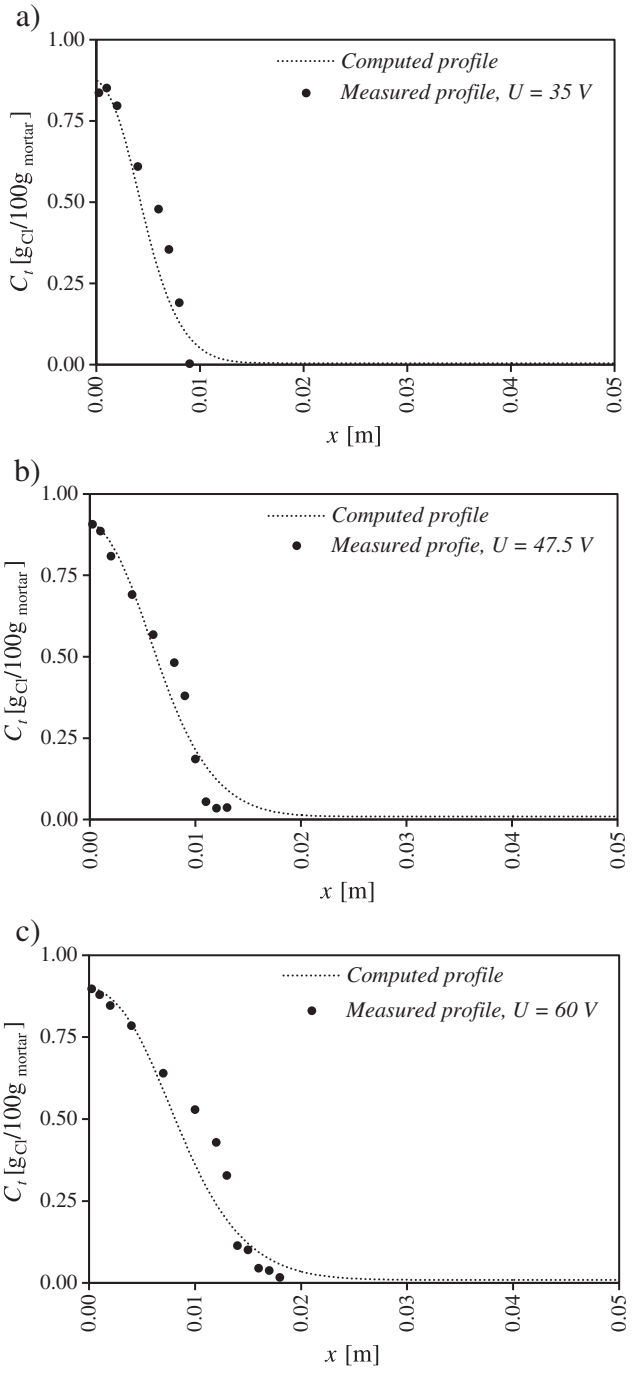

Fig. 15. Total chloride concentration profiles computed from the new chloride transport model given in [3]: a) 35 V; b) 47.5 V; c) 60 V; vs. measured values.

4. Conclusions

The influence of the applied voltage on the chloride migration coefficient in mortars was investigated in this study. For the 'traditional' RCM test model, the obtained D_{RCM} coefficient was about 10% larger for samples tested at 60 V compared to samples tested at lower voltages (35 V and 47.5 V). For the new RCM model, which is considering the non-linear binding isotherm and non-equilibrium between free- and bound-chlorides concentrations, no trends were observed for the obtained D_{eff} coefficients. Therefore, it can be concluded that the voltage in the investigated range is not influencing the chloride migration coefficients significantly.

As also demonstrated, the guideline for the RCM test [1] may not specify correctly the test conditions for the mortar that was tested in this study—the applied voltage suggested by NT Build 492 resulted in shallow chloride penetration depths, which reduces the precision of the calculated D_{RCM} value. However, it has to be indicated, that the recommendations for the test conditions given in [1] are based on the experience with OPC concrete only.

A dark coloration was observed on all split samples after the RCM test prior to spraying with $AgNO_3$. The thickness of this region was comparable to the measured chloride penetration depth. This effect may be caused by an incomplete liquid saturation of the samples during the vacuum-saturation and/or by water transport due to the electrical field. Further research is therefore needed in order to verify the

effectiveness of the vacuum-saturation technique recommended by the guidelines and to study the electro-osmosis during the migration tests.

As also demonstrated, the properties of the mortar and the electrolytes change during the RCM test. The increasing resistance of the samples was the reason of decreasing currents, which was observed during all the experiments. However, the evolution of the current at 60 V was somewhat different compared to lower voltages. Changes of the mass and resistance before and after the application of the electrical field were observed on the test samples. The mass increase was found to be proportional to the chloride penetration depth and the resistance was found to be increased with about 25% after the test, regardless of the value of the applied voltage. The pH of the catholyte solution increased significantly during the RCM test. This means that, with time, a larger fraction of the current flows in the system due to OH^- migration instead of the Cl^- migration. The influence of these non-constant properties of the samples and changing test conditions on the migration test needs to be further investigated.

The measured polarization of the stainless-steel electrodes confirmed the value of 2 V assumed in the NT Build 492 [1]. Additionally, the polarization of titanium based electrodes was measured, as the titanium is a better suited material to be used as electrode.

List of symbols

Roman		
a	Migration constant $a = zF(U-2)/(RTL)$	[1/m]
c	Free-chloride concentration	[g_{Cl}/$dm^3_{solution}$]
c_d	Minimum free-chloride concentration detected with 0.1 M $AgNO_3$	[g_{Cl}/$dm^3_{solution}$]
c_0	Free-chloride concentration in bulk solution	[g_{Cl}/$dm^3_{solution}$]
c_b	Bound-chlorides concentration	[g_{Cl}/$dm^3_{solution}$]
C_b	Bound-chlorides concentration	[g_{Cl}/g_{mortar}]
C_{bi}	Initial bound-chlorides concentration	[g_{Cl}/g_{mortar}]
C_t	Total concentration of chlorides	[g_{Cl}/100 g_{mortar}]
COV	Coefficient of variation	[%]
D	Chloride diffusion coefficient	[m^2/s]
D_0	Intrinsic chloride diffusion coefficient [4]	[m^2/s]
D_{eff}	Effective chloride migration coefficient [3]	[m^2/s]
D_{RCM}	Apparent chloride migration coefficient [1,4]	[m^2/s]
f	Frequency	[Hz]
F	Faraday constant	[C/mol]
h	Height of mortar sample	[cm]
I	Current	[mA]
I_0	Initial current during the RCM test	[mA]
I_{30}	Current measured at $U = 30$ V	[mA]
I_f	Final current during the RCM test	[mA]
k	Chloride mass transfer coefficient	[1/s]
K_b	Chloride binding capacity	[dm^{3n}/g^n]
L	Thickness of specimen	[m]
m_{Cl}	Mass of chloride	[g]
m_d	Mass of dried sample	[g]
m_{OH}	Mass of hydroxyl ions	[g]
m_s	Mass of water-saturated sample measured in air	[g]
m_w	Mass of water-saturated sample measured in water	[g]
n	Chloride binding intensity parameter	–
n_{Cl}	Moles of chlorides	[mol]
n_{OH}	Moles of hydroxyls	[mol]
R	Universal gas constant	[$Jmol^{-1}K^{-1}$]
t	Time	[s] or [h]
t_{RCM}	Duration of the RCM test	[s]
T	Temperature	[K]
U	Voltage	[V]
x	Distance	[m] or [mm]
x_d	Chloride penetration depth	[m] or [mm]
z	Ion valence	–
Greek		
α	Laboratory constant for the RCM test	–
φ	Total water-accessible porosity of mortar	–
Φ	Diameter of cylindrical mortar sample	[cm]
ρ_c	Apparent density of liquid-saturated mortar	[g/dm^3]
ρ_d	Apparent density of dry mortar	[g/dm^3]
ρ_s	Specific density of mortar	[g/dm^3]
Δm	Mass difference of the sample prior to and after the RCM test	[g]

Acknowledgments

The authors wish to express their gratitude to ir. J.J.W. Gulikers (Rijkswaterstaat Centre for Infrastructure, Utrecht, the Netherlands) for his advice and support of this research, to Dipl. -Ing. Ch. Helm (IBAC, RWTH Aachen, Germany) for performing the polarization measurements, to Dipl. Eng. M.V.A. Florea (TU Eindhoven) for her help and to the following sponsors of the Building Materials research group at TU Eindhoven: Rijkswaterstaat Centre for Infrastructure, Graniet-Import Benelux, Kijlstra Betonmortel, Struyk Verwo, Attero, Enci, Provincie Overijssel, Rijkswaterstaat Directie Zeeland, A&G Maasvlakte, BTE, Alvon Bouwsystemen, V.d. Bosch Beton, Selor, Twee "R" Recycling, GMB, Schenk Concrete Consultancy, Intron, Geochem Research, Icopal, BN International, APP All Remove, Consensor, Eltomation, Knauf Gips, Hess ACC Systems and Kronos (chronological order of joining).

References

[1] NT Build 492, Concrete, mortar and cement-based repair materials: chloride migration coefficient from non-steady-state migration experiments, Nordtest method, 1999.
[2] DuraCrete, Probabilistic performance based durability design of concrete structures, DuraCrete Final Technical Report, 2000, Document BE95–1347/R17.
[3] P. Spiesz, M.M. Ballari, H.J.H. Brouwers, RCM: a new model accounting for the non-linear chloride binding isotherm and the non-equilibrium conditions between the free- and bound-chloride concentrations, Constr. Build. Mater. 27 (2012) 293–304.
[4] L. Tang, Chloride transport in concrete—measurement and prediction. PhD Thesis, 1996, Chalmers University of Technology, Gothenburg, Sweden.
[5] L. Tong, O.E. Gjørv, Comparison of the sensitivities between non-steady and steady state migration test methods, Proceedings of the Nordtest mini-seminar on chloride diffusion coefficient of concrete and relevant test methods, Nordtest Project No. 1351–97, May 1997, Borås, Sweden, 1997.
[6] K.D. Stanish, R.D. Hooton, M.D.A. Thomas, Prediction of chloride penetration in concrete, US Department of Transportation, Federal Highway Administration, 2001 FHWA-RD-00-142.
[7] K.D. Stanish, The migration of chloride ions in concrete. PhD Thesis, 2002, University of Toronto, Canada.
[8] ASTM C 1202–05, Standard Test Method for Electrical Indication of Concrete's Ability to Resist Chloride Ion Penetration, 2005.
[9] P.F. McGrath, R.D. Hooton, Influence of voltage on chloride diffusion coefficients from chloride migration tests, Cem. Concr. Res. 26 (1996) 1239–1244.
[10] ASTM C 642–97, Standard Test Method for Density, Absorption, and Voids in Hardened Concrete, 1997.
[11] BAW-Merkblatt, Chlorideindringwiderstand, Bundesanstalt für Wasserbau, 2004 (in German).
[12] H.G. Midgley, J.M. Illston, The penetration of chlorides into hardened cement pastes, Cem. Concr. Res. 14 (1984) 546–558.
[13] H. Hornain, J. Marchand, V. Duhot, M. Moranville-Regourd, Diffusion of chloride ions in limestone filler blended cement pastes and mortars, Cem. Concr. Res. 25 (8) (1995) 1667–1678.
[14] C. Andrade, Calculation of chloride diffusion coefficients in concrete from ionic migration measurements, Cem. Concr. Res. 23 (1993) 724–742.
[15] L. Tang, L.-O. Nilsson, Rapid determination of the chloride diffusivity in concrete by applying an electrical field, ACI Mater. J. 89 (1992) 49–53.
[16] L. Tang, L.-O. Nilsson, A new approach to the determination of pore distribution by penetrating chlorides into concrete, Cem. Concr. Res. 25 (1995) 695–701.
[17] E. Gruyaert, Ph. Van den Heede, N. De Beile, Chloride ingress for concrete containing blast-furnace slag, related to microstructural parameters, Proceedings of the 2nd International RILEM Workshop on Concrete Durability and Service Life Planning, RILEM Publications S.A.R.L., Haifa, Israel, 2009, pp. 440–448.
[18] M. Castellote, C. Andrade, C. Alonso, Chloride-binding isotherms in concrete submitted to non-steady-state migration experiments, Cem. Concr. Res. 29 (1999) 1799–1806.
[19] M. Castellote, C. Andrade, C. Alonso, Accelerated simultaneous determination of the chloride depassivation threshold and of the non-stationary diffusion coefficient values, Corros. Sci. 44 (2002) 2409–2424.

[20] Q. Yuan, Fundamental studies on test methods for the transport of chloride ions in cementitious materials. PhD Thesis, 2009, University of Ghent, Belgium.
[21] C.C. Yang, C.T. Chiang, Relation between the chloride migration coefficients of concrete from the colourimetric method and the chloride profile method, J. Chin. Inst. Eng. 32 (2009) 801–809.
[22] C. Andrade, M. Castellote, C. Alonso, C. González, Relation between colourimetric chloride penetration depth and charge passed in migration tests of the type of standard ASTM C1202-91, Cem. Concr. Res. 29 (1999) 417–421.
[23] P.A. Claisse, H.I. Elsayad, E. Ganjian, Modelling the rapid chloride permeability test, Cem. Concr. Res. 40 (2010) 405–409.
[24] N. Otsuki, S. Nagataki, K. Nakashita, Evaluation of $AgNO_3$ solution spray method for measurements of chloride penetration into hardened cementitious matrix materials, ACI Mater. J. 89 (6) (1992) 587–592.